Mediterranean Journal of Hematology and Infectious Diseases

Original Article

Association Between Pre-Admission 48-Hour Fever Burden and Outcomes in Pediatric Mycoplasma Pneumoniae Infection

Lijie Ma[1] and Ling Chen[1].

[1] Children's Comprehensive Department, The Second Affiliated Hospital of Guangdong Medical University, Zhanjiang, Guangdong 524000 China.

Competing interests: The authors declare no competing interest.

Abstract. ***Background:*** **Refractory and severe evolution complicate pediatric Mycoplasma pneumoniae pneumonia (MPP), yet early risk stratification still relies largely on single-time admission biomarkers. We tested whether a prespecified 48-hour pre-admission fever-burden index (FBI48) predicts in-hospital outcomes and improves model performance beyond guideline-consistent clinical and laboratory predictors.**

Methods**: We conducted a retrospective single-center cohort study of hospitalized children ≤14 years with laboratory-confirmed MPP. FBI48 was defined as the area under the temperature–time curve above 38.0 °C over −48 to 0 h (°C·h). Thresholds of 38.5 °C and 39.0 °C were evaluated in sensitivity analyses. Prespecified covariates, chosen based on prior RMPP/SMPP studies and pediatric CAP/MPP guidelines, included age, illness days, SpO2, imaging severity, prior macrolide exposure, antipyretic and steroid use, LDH, log2-transformed NLR, CRP, and PCT. Penalized logistic regression generated predicted risks, while unpenalized models provided adjusted odds ratios. Model performance (AUC, Brier score, calibration) and decision-curve analysis (DCA) net benefit were assessed for base (clinical + laboratory) and augmented (base + FBI48) models across 10–30% risk thresholds.**

Results**: Of 720 eligible hospitalizations, 648 were analyzed. The composite endpoint (RMPP and/or incident SMPP) occurred in 176/648 (27.2%; RMPP 24.7%; SMPP 8.0%). FBI48 was independently associated with the composite endpoint (adjusted odds ratio [aOR] 1.45, 95% CI 1.25–1.68 per 1 SD ≈22 °C·h) and with SMPP alone (aOR 1.58, 95% CI 1.21–2.06). Adding FBI48 to the base model improved AUC from 0.78 to 0.83 (ΔAUC 0.05, p<0.001), reduced the Brier score (0.176 to 0.164, p=0.006), and increased net benefit compared with the base model and a treat-none strategy across 10–30% thresholds. Alternative fever thresholds (38.5 °C/39.0 °C) yielded similar effect sizes.**

Conclusions**: A simple 48-hour pre-admission fever-burden metric provides independent and incremental prognostic information on the risk of refractory or severe evolution in pediatric MPP, complementing guideline-based clinical and laboratory predictors and supporting admission-time risk stratification. External validation and prospective evaluation of dynamic, in-hospital updating are warranted.**

Keywords: Mycoplasma pneumoniae pneumonia; Fever-bourden Index; Prognosis; Fever threshold.

Citation: Ma L., Chen L. Association between pre-admission 48-hour fever burden and outcomes in pediatric mycoplasma pneumoniae infection. Mediterr J Hematol Infect Dis 2026, 18(1): e2026034, DOI: http://dx.doi.org/10.4084/MJHID.2026.034

Published: May 01, 2026 **Received: December 01, 2025** **Accepted: April 02, 2026**

Correspondence to: Lijie Ma. No.12 Minyou Road, Xiashan District, Zhanjiang City, Guangdong Province, 524000. E-mail: LijieMa654@163.com

Introduction. Mycoplasma pneumoniae pneumonia (MPP) in children can progress to refractory (RMPP) or severe (SMPP) forms. Traditional reliance on single-time biomarkers such as C-reactive protein (CRP) and procalcitonin (PCT) may not fully capture the disease's dynamic nature before hospital admission. Recent studies have identified several biomarkers and clinical indicators that can aid in early prediction and management of RMPP and SMPP. Elevated levels of CRP, lactate dehydrogenase (LDH), and D-dimer have been consistently associated with RMPP.[1-4] Additionally, inflammatory cytokines such as interleukin-6 (IL-6) and tumor necrosis factor-alpha (TNF-α) have been linked to severe MPP.[3] Logistic regression models have further highlighted the importance of factors such as prolonged fever duration, high peak body temperature, and specific radiological features, such as large lobar consolidation, in predicting RMPP.[2,5] Moreover, the presence of macrolide-resistant Mycoplasma pneumoniae strains and excessive host immune responses are significant contributors to the refractory nature of the disease.[6] A dynamic nomogram incorporating multiple risk factors, including age, neutrophil-to-lymphocyte ratio, and pleural effusion, has been developed to enhance the accuracy of SMPP predictions.[7] Existing prognostic models for pediatric MPP typically rely on admission-time snapshots (e.g., LDH, CRP, NLR) and simple fever descriptors (e.g., duration or peak temperature), but rarely quantify the cumulative pre-admission fever trajectory, integrating intensity and duration into a standardized dynamic measure.[2,5,7] Accordingly, an unresolved gap is whether a prespecified 48-hour fever-burden metric provides incremental prognostic value beyond routine admission predictors and imaging severity.

The pre-admission 48-hour fever-burden index (FBI48) is a comprehensive metric that quantifies the intensity and duration of fever prior to hospital admission. This index is particularly relevant as fever is a critical component of the host's immune response, enhancing the efficacy of immune cells and exerting stress on pathogens.[8] Observational studies have shown that fever trajectories correlate with distinct immune profiles and clinical outcomes.[9] Moreover, the concept of a fever index, which integrates both the height and duration of fever, has been previously validated in clinical settings.[10] Thus, the FBI48 could provide a more nuanced understanding of febrile responses, aiding in clinical decision-making and management strategies.[11,12]

The question of whether the FBI48 model predicts RMPP/SMPP independently and adds value to routine admission predictors is underscored by the evolving landscape of predictive analytics in healthcare. Current models emphasize integrating multiple risk factors to improve predictive accuracy. More broadly, routine admission laboratory tests can add prognostic information in acute illness prediction models.[13] In pediatric MPP, multivariable tools increasingly integrate routine admission laboratories with clinical and radiographic features to support early risk stratification.[2,7,14] Furthermore, machine learning techniques are increasingly utilized to analyze extensive patient datasets. Thus, while the FBI48 model's independent predictive capability remains to be fully established, integrating diverse predictors, including those from routine admissions, is crucial for improving overall prediction accuracy in clinical settings.[15,16]

We hypothesize that dynamic pre-admission fever patterns encode clinically relevant information about host–pathogen inflammatory activity and that a 48-hour fever-burden index (FBI48) would identify children at heightened risk for complicated courses of MPP. Our primary objective was to test the association between FBI48 and a composite endpoint comprising RMPP and/or SMPP occurring during hospitalization. Secondary objectives were to evaluate the association of FBI48 with SMPP alone and to determine whether FBI48 provides incremental prognostic value beyond a prespecified base model that includes guideline-consistent clinical features and routine admission laboratory values.

Methods

Study design and setting. We conducted a retrospective, single-center observational cohort study at The Second Affiliated Hospital of Guangdong Medical University from October 2021 through August 2025, using routinely collected data on consecutive hospitalizations of children aged ≤14 years with laboratory-confirmed MPP. Admission was the index time. All exposures and covariates were defined at or prior to admission, and outcomes were ascertained during the index hospitalization. This study was conducted in accordance with the Declaration of Helsinki. The protocol was reviewed and approved by the Ethics Committee of The Second Affiliated Hospital of Guangdong Medical University, which waived the requirement for informed consent because the study was a retrospective analysis of de-identified, routinely collected data and posed no more than minimal risk to participants. All data were anonymized prior to analysis.

Participants and cohort assembly. We screened consecutive admissions for suspected community-acquired pneumonia with testing for M. pneumoniae. Inclusion required laboratory-confirmed MPP, analyzable pre-admission temperature data spanning −48 to 0 hours, and a complete admission laboratory panel.

To preserve an incident assessment of in-hospital progression, children who met SMPP criteria at presentation were excluded from endpoint evaluation.

Diagnostic criteria and respiratory sampling. Diagnostic criteria for MPP were aligned with the 2023 evidence-based guideline for pediatric MPP and pediatric CAP guidance. MPP required compatible clinical and radiographic findings plus either a positive respiratory nucleic-acid amplification test (NAAT/PCR) for M. pneumoniae from throat or nasopharyngeal swab, or a ≥4-fold rise in M. pneumoniae-specific antibody titer between acute and convalescent sera when NAAT was unavailable. Genotypic macrolide resistance testing for *M. pneumoniae* was not routinely performed during the study period; therefore, isolate-level resistance rates were unavailable for analysis.

48-hour pre-admission fever-burden index (FBI48). The primary exposure was FBI48, defined as the area under the temperature–time curve above a prespecified fever threshold T0 over the 48 h before admission, where T(t) is the recorded body temperature at time t (hours) relative to admission (t=0), with T0=38.0 °C as primary and 38.5 °C/39.0 °C in sensitivity analyses. An analyzable pre-admission temperature window required ≥4 timestamped temperature measurements between -48 and 0 h (including ≥1 within -6 h) and no single gap between adjacent measurements >18 h; windows not meeting these criteria were classified as non-analyzable and excluded.

Temperatures were abstracted from outpatient and emergency department records and caregiver logs, converted to degrees Celsius, time-aligned to admission (t = 0), and deduplicated. Because sampling times were irregular, we linearly interpolated between successive observations and applied the trapezoidal rule within the observed time span. We did not extrapolate beyond the earliest or latest measurements in the −48 to 0 h window. When the measurement site/device was documented, we retained the recorded value without applying site-specific offsets; robustness to potential misclassification was partly assessed by repeating FBI48 computations at higher fever thresholds (38.5°C and 39.0°C). When multiple measurements occurred within ±15 minutes, we deduplicated by retaining the highest value and the earliest timestamp. When outpatient/ED records and caregiver logs overlapped within ±30 minutes, we prioritized the clinical record.

Outcomes and clinical definitions. The primary endpoint was a composite of RMPP and/or incident SMPP during the index hospitalization among children who were not SMPP at presentation. RMPP was defined in accordance with contemporary guidelines as persistent fever with non-improving or worsening lung imaging despite ≥7 days of appropriate macrolide therapy. SMPP was defined for MPP cases that met recognized severe pediatric CAP criteria, operationalized as any of the following developing after admission: hypoxemia (SpO2 <92% on room air at sea level or need for supplemental oxygen to maintain SpO2 ≥92%), need for advanced respiratory support (high-flow nasal cannula, noninvasive ventilation, or invasive mechanical ventilation), multilobar consolidation and/or moderate-to-large pleural effusion, ICU/HDU transfer for respiratory support, or clinically significant extrapulmonary involvement as documented by the treating team (e.g., neurologic, cardiovascular, hepatic, or dermatologic complications). Only SMPP developing after admission contributed to endpoints. SMPP was present at the presentation. SMPP alone served as a secondary endpoint. All outcomes were adjudicated using prespecified definitions prior to model fitting.

Covariates, imaging, and laboratory preprocessing. Prespecified covariates at admission included age (years), illness days (days since symptom onset), peripheral oxygen saturation by pulse oximetry (SpO2, %), chest radiograph severity (mild vs moderate/severe by standardized reading of the admission film), prior macrolide exposure before admission (yes/no), antipyretic exposure during −48 to 0 h (yes/no), and pre-admission systemic steroid exposure (yes/no). These variables were chosen a priori based on prior RMPP/SMPP prognostic studies and pediatric MPP/CAP guidelines, rather than by data-driven selection. Radiograph severity was categorized as mild versus moderate/severe based on prespecified criteria (extent of consolidation, multilobar involvement, and/or pleural effusion) abstracted from the admission radiology report; ambiguous cases were adjudicated by a second reviewer.

Admission laboratory values were obtained within 6 hours of arrival: LDH (U/L), NLR, CRP (mg/L), and PCT (ng/mL). For modeling, LDH was scaled to 100 U/L, NLR was log2-transformed, CRP was modeled per 10 mg/L, and PCT was modeled per 0.1 ng/mL. As noted, continuous covariates were centered and standardized to aid interpretation. Other potential biomarkers were not included as predictors because they were not routinely measured at admission or exhibited >30% missingness, which would compromise model stability. Chest computed tomography was not routinely performed and was reserved for suspected complications. Modeling used the admission radiograph category to preserve general applicability.

Missing data and imputation. We examined missingness patterns after exclusions and used multiple imputation by chained equations (MICE) under a Missing-at-Random assumption, including all model variables and the

outcome to preserve associations. Because a complete admission laboratory panel was required for inclusion, LDH, NLR, CRP, and PCT were not imputed. The remaining missingness was confined to a small fraction of the clinical covariates. We imputed continuous variables using predictive mean matching (age, illness days, SpO2) and binary variables using logistic regression (imaging severity, prior macrolide exposure, antipyretic exposure, and pre-admission systemic steroid exposure). Twenty imputations were generated with convergence checks, and Rubin's rules were used to combine estimates. Variables with substantial missingness (>30%) were not included in the model. Children with no usable −48 to 0 h temperature data or without a complete admission laboratory panel were excluded a priori

Statistical analysis. Baseline characteristics were summarized overall and by the composite endpoint using means with standard deviations or medians with interquartile ranges, and compared using Wilcoxon rank-sum tests for continuous variables and $\chi 2$ (or Fisher's exact) tests for categorical variables. Benjamini–Hochberg false-discovery-rate (FDR) q-values were reported. These baseline comparisons were descriptive; primary inference regarding prognostic associations relied on prespecified multivariable models.

Prediction used penalized logistic regression (ridge/elastic-net tuned by cross-validation) to mitigate overfitting and collinearity, while unpenalized logistic models on the imputed datasets provided adjusted odds ratios (aORs) with 95% CIs and p-values for clinical interpretability. For the composite endpoint and the SMPP endpoint, model complexity was deliberately limited to maintain a reasonable events-per-variable ratio, with penalization further constraining overfitting. For penalized models, we used 10-fold cross-validation to tune the elastic-net mixing parameter α (grid 0.0-1.0 in 0.1 increments) and the penalty λ, selecting λ by the 1-SE rule. For primary inferential and prediction models, FBI48 was entered as a standardized linear term. Restricted cubic splines were used in a prespecified secondary analysis to assess nonlinearity. With 176 composite events and 12 prespecified predictors, the events-per-predictor (EPV) was 14.7. The SMPP model used 6 predictors for 52 events (EPV 8.7) and therefore relied on penalization and bootstrap internal validation. Other continuous covariates used linear or log-linear forms as specified.

Penalized models were used to generate predicted probabilities in each imputed dataset. Discrimination (AUC with 95% CI by DeLong), calibration (intercept and slope), and overall accuracy (Brier score) were calculated from these predictions and pooled across imputations. Bootstrap optimism-correction was applied for internal validation. Decision-curve analysis (DCA) quantified net benefit over 10–30% risk thresholds chosen a priori for forward escalation decisions, comparing a base model (clinical features + routine laboratories) against an augmented model (base + FBI48) and a treat-none strategy. Two-sided $\alpha = 0.05$ defined statistical significance. For incremental performance metrics, 95% CIs for ΔAUC were obtained using DeLong's method, and 95% CIs for ΔBrier were obtained by bootstrap resampling.

Sensitivity analyses. To assess the robustness of the FBI48 exposure definition, we recomputed the integral using fever thresholds of 38.5 °C and 39.0 °C, with the same prespecified covariate set, and refit the models. We summarized the FBI48 aOR per 1 SD for each threshold and qualitatively compared model performance with the primary specification, without re-tuning variable selection to avoid overfitting to any single definition. FBI48 tertiles were used solely for descriptive event-rate summaries and not for model fitting.

Results.

Cohort assembly and event rates. Of 720 eligible hospitalizations during October 2021 to August 2025, 648 children met inclusion criteria (available −48 to 0 h temperatures and admission laboratories) and comprised the analysis cohort after excluding 30 with missing pre-admission temperatures, 17 with missing admission laboratories, and 25 with SMPP at presentation (**Figure 1**). Within the analysis cohort, the composite endpoint of RMPP and/or incident SMPP occurred in 176/648 (27.2%, 95% CI 23.8–30.6), including RMPP in 160 (24.7%, 95% CI 21.4–28.0) and SMPP in 52 (8.0%, 95% CI 6.0–10.1); 36 children met both outcomes (**Table 1, Figure 1**).

At admission, the cohort had a mean age of 6.8 ± 2.9 years, median illness days 4.8 [3.0–6.0], and median FBI48 46 [33–58] °C·h (**Table 1**). In the -48 to 0 h window, children had a median of 7 [5–10] temperature measurements; the median maximum inter-measurement gap was 7.0 [4.5–10.5] h. Overall, 59.0% of temperature readings were sourced from outpatient/ED records and 41.0% from caregiver logs (**Supplementary Table S1**).

Included (n=648) and excluded eligible hospitalizations (n=72) showed similar distributions of age, sex, illness days, admission SpO2, and imaging severity, supporting limited selection bias from the analyzable-temperature and laboratory-panel requirements (**Supplementary Table S2)**.

Baseline characteristics by outcome. Compared with children without events, those with the composite endpoint were older (7.6 ± 2.9 vs 6.5 ± 2.9 years; p=0.004, q=0.012) and presented later in their illness (5.2 [4.0–6.5] vs 4.6 [3.0–6.0] days; p=0.010, q=0.018). They had lower admission SpO2 (95.1 ± 2.6% vs 97.0 ± 2.1%;

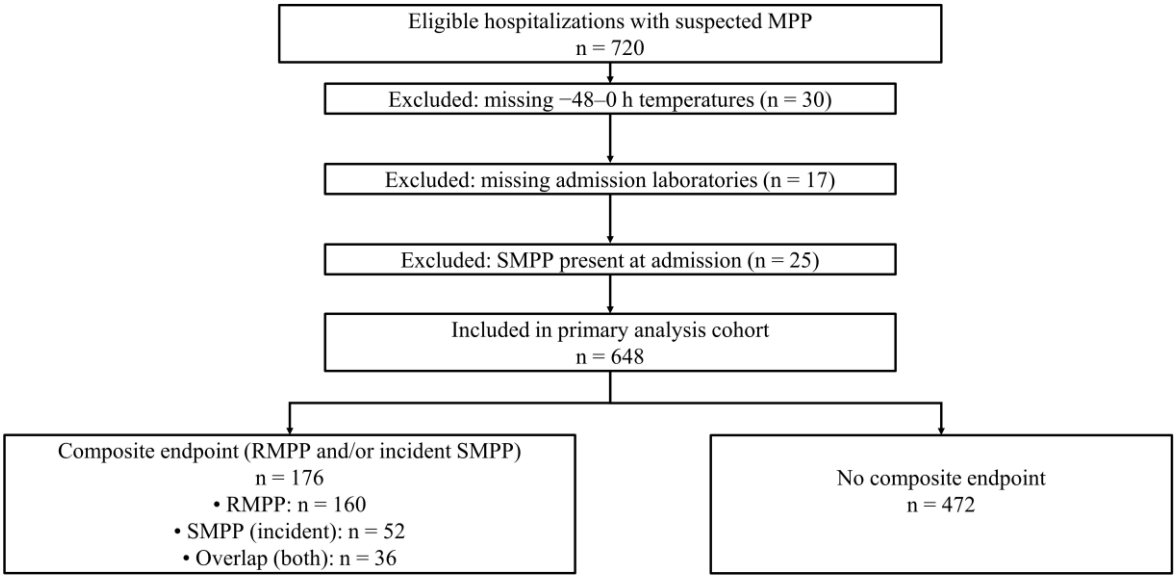

Figure 1. Study flow diagram. Flow of cohort assembly for hospitalized children ≤14 years with laboratory-confirmed MPP.

Table 1. Baseline characteristics overall and by composite endpoint.

Variable	Overall	No composite event (n=472)	Composite event (n=176)	p	q (FDR)
Age, y (mean ± SD)	6.8 ± 2.9	6.5 ± 2.9	7.6 ± 2.9	0.004	0.012
Male, n (%)	337 (52.0%)	240 (50.8%)	97 (55.1%)	0.24	0.32
Illness days at admission (median [IQR])	4.8 [3.0–6.0]	4.6 [3.0–6.0]	5.2 [4.0–6.5]	0.010	0.018
SpO_2 at admission, % (mean ± SD)	96.4 ± 2.4	97.0 ± 2.1	95.1 ± 2.6	<0.001	<0.001
Imaging severity (moderate/severe), n (%)	241 (37.2%)	144 (30.5%)	97 (55.1%)	<0.001	<0.001
Prior macrolide exposure, n (%)	155 (23.9%)	104 (22.0%)	51 (29.0%)	0.060	0.100
Antipyretic exposure (−48 to 0 h), n (%)	423 (65.3%)	298 (63.1%)	125 (71.0%)	0.058	0.098
Steroid exposure (pre-admission), n (%)	40 (6.2%)	24 (5.1%)	16 (9.1%)	0.080	0.110
LDH, U/L (median [IQR])	345 [288–420]	318 [266–384]	412 [351–476]	<0.001	<0.001
NLR (median [IQR])	4.1 [2.8–6.1]	3.6 [2.5–5.1]	5.1 [3.7–7.2]	<0.001	<0.001
CRP, mg/L (median [IQR])	21 [11–36]	18 [9–31]	26 [14–47]	<0.001	<0.001
PCT, ng/mL (median [IQR])	0.14 [0.07–0.28]	0.12 [0.06–0.24]	0.20 [0.09–0.36]	0.002	0.006
FBI48, °C·h (median [IQR])	46 [33–58]	43 [30–55]	57 [44–74]	<0.001	<0.001

p<0.001, q<0.001) and more frequent moderate/severe radiographic involvement (55.1% vs 30.5%; p<0.001, q<0.001), and showed higher inflammatory/injury markers, including LDH (412 [351–476] vs 318 [266–384] U/L; p<0.001, q<0.001), NLR (5.1 [3.7–7.2] vs 3.6 [2.5–5.1]; p<0.001, q<0.001), CRP (26 [14–47] vs 18 [9–31] mg/L; p<0.001, q<0.001), and PCT (0.20 [0.09–0.36] vs 0.12 [0.06–0.24] ng/mL; p=0.002, q=0.006). FBI48 was higher among event cases (57 [44–74] vs 43 [30–55] °C·h; p<0.001, q<0.001). Event rates rose stepwise across FBI48 tertiles from 16.7% and 3.7% in the lowest tertile (≤32 °C·h) to 40.3% and 13.9% in the highest (≥56 °C·h) for the composite endpoint and SMPP, respectively (**Supplementary Table S3 and Figure 2**).

Primary multivariable analysis (composite endpoint). In multivariable logistic models on multiply imputed data, higher FBI48 remained independently associated with the composite endpoint with an aOR of 1.45 (95% CI 1.25–1.68) per 1 SD (~22 °C·h) increase (**Table 2**). Additional predictors of higher odds included older age (aOR 1.06 per 1 year, 95% CI 1.02–1.10), more illness

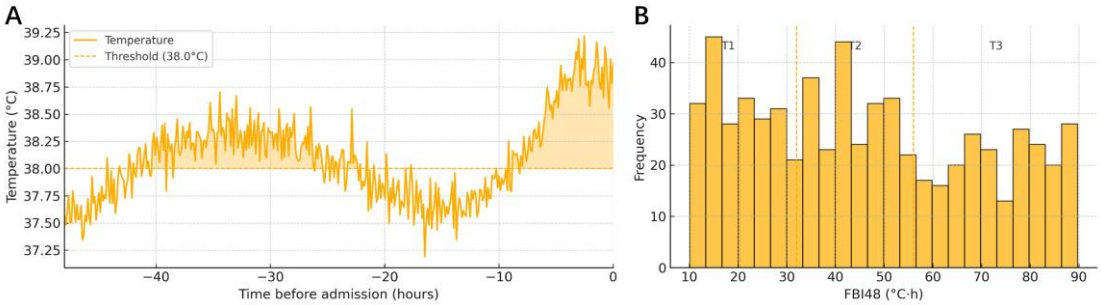

Figure 2. FBI48 construct and distribution. (A) Schematic showing the FBI48 as the area under the temperature curve above a prespecified threshold of 38.0 °C over −48 to 0 hours (shaded). **(B)** Distribution of FBI48 in the analysis cohort (n=648) with tertile cut-points marked at ≤32 °C·h (T1), 33–55 °C·h (T2), and ≥56 °C·h (T3).

Table 2. Composite endpoint for Multivariable models.

Predictor (scaling)	Adjusted OR (95% CI)	p	q (FDR)
FBI48 (per 1 SD ≈ 22 °C·h)	1.45 (1.25–1.68)	<0.001	<0.001
Age (per 1 y)	1.06 (1.02–1.10)	0.004	0.012
Illness days (per 1 d)	1.08 (1.02–1.15)	0.008	0.018
SpO2 (per 1% lower)	1.12 (1.07–1.18)	<0.001	<0.001
Imaging severity (mod/severe vs mild)	1.92 (1.31–2.80)	0.001	0.005
LDH (per 100 U/L higher)	1.11 (1.05–1.18)	<0.001	0.002
NLR (log-transformed, per 1 unit)	1.28 (1.12–1.47)	<0.001	0.003
CRP (per 10 mg/L)	1.08 (1.03–1.13)	0.002	0.009
PCT (per 0.1 ng/mL)	1.04 (1.00–1.08)	0.048	0.072
Prior macrolide (yes vs no)	1.23 (0.87–1.73)	0.24	0.30
Antipyretic exposure (yes vs no)	1.19 (0.86–1.64)	0.29	0.34
Steroid exposure (yes vs no)	1.46 (0.76–2.76)	0.25	0.31

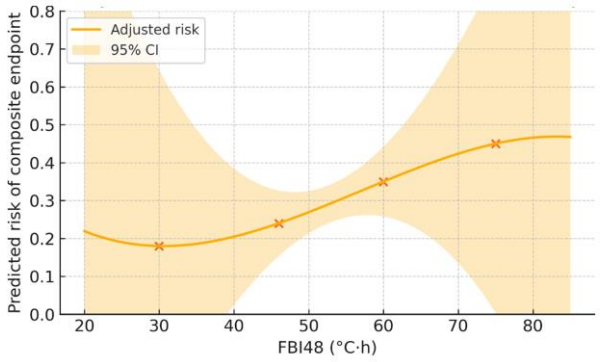

Figure 3. Adjusted association of FBI48 with risk of the composite endpoint. Adjusted predicted risk of RMPP and/or incident SMPP across FBI48 values from a multivariable logistic model including FBI48 (restricted cubic splines) and prespecified covariates (age, illness days, SpO_2, imaging severity, prior macrolide, antipyretic/steroid exposure, LDH, log_2-NLR, CRP, and PCT). The solid line shows the point estimate and the shaded band the 95% CI. (Spline specification: restricted cubic spline with 4 knots at the 5th, 35th, 65th, and 95th percentiles of FBI48; shown for nonlinearity assessment and visualization).

days at admission (aOR 1.08 per 1 day, 95% CI 1.02–1.15), lower SpO2 (aOR 1.12 per 1% lower, 95% CI 1.07–1.18), moderate/severe imaging (aOR 1.92, 95% CI 1.31–2.80), LDH (aOR 1.11 per 100 U/L, 95% CI 1.05–1.18), NLR (aOR 1.28 per log2 unit, 95% CI 1.12–1.47), and CRP (aOR 1.08 per 10 mg/L, 95% CI 1.03–1.13), whereas PCT showed a borderline association (aOR 1.04 per 0.1 ng/mL, 95% CI 1.00–1.08). After Benjamini–Hochberg adjustment, FBI48, SpO2, imaging severity, LDH, NLR, and CRP remained significant (q≤0.01), while prior macrolide, antipyretic, and pre-admission steroid exposure were not independently associated (q≥0.30).

In a prespecified secondary analysis, restricted cubic spline modeling supported a monotonic, mildly nonlinear FBI48–risk relationship (likelihood-ratio test for nonlinearity p=0.028), with adjusted risks of approximately 18% (95% CI 14–23), 24% (21–28), 35% (29–41), and 45% (36–53) at FBI48 values of 30, 46, 60, and 75 °C·h, respectively (**Figure 3**).

Incremental value and internal validation (composite endpoint). Adding FBI48 to the clinical + laboratory base model improved discrimination from an AUC of 0.78 (95% CI 0.74–0.81) to 0.83 (95% CI 0.80–0.86), ΔAUC = 0.05 (DeLong p<0.001), with optimism-corrected AUCs of 0.77 and 0.82, respectively (**Figure 4A and Table 3**). Calibration improved concurrently (slope 0.94 [95% CI 0.82–1.06] to 1.02 [0.91–1.13]; intercept −0.04 to −0.01), and overall accuracy improved, as reflected by

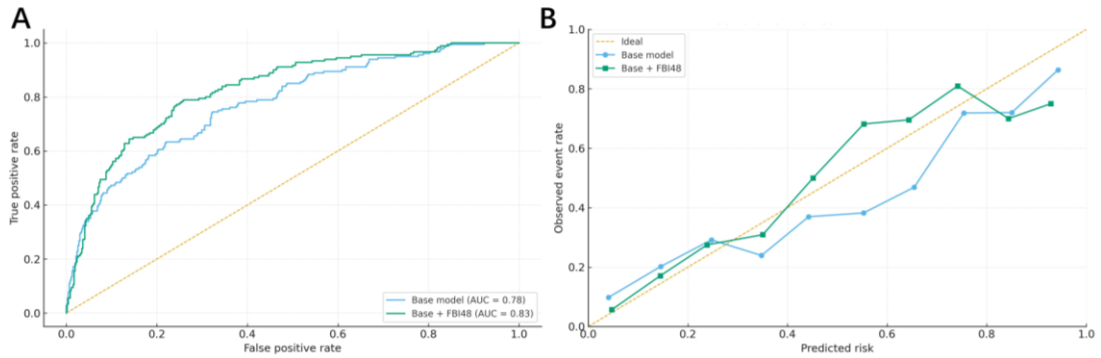

Figure 4. Model performance for the composite endpoint. (A) ROC curves comparing a base model (clinical features + routine laboratories) with the base model plus FBI48. **(B)** Calibration plots showing the ideal line (y = x) and the apparent calibration for each model. Calibration in panel B uses 10 equal-frequency bins of predicted risk with a smoother loss.

Table 3. Model performance.

Metric	Base (clinical + labs)	Base + FBI48	Δ (Base → +FBI48)
AUC (95% CI)	0.78 (0.74–0.81)	0.83 (0.80–0.86)	+0.05, p<0.001 (DeLong)
AUC, optimism-corrected	0.77	0.82	+0.05
Calibration slope (95% CI)	0.94 (0.82–1.06)	1.02 (0.91–1.13)	+0.08
Calibration intercept (95% CI)	−0.04 (−0.12 to 0.05)	−0.01 (−0.09 to 0.08)	+0.03
Brier score	0.176	0.164	−0.012, p=0.006
Net benefit at 10% threshold	0199	0.215	+0.016
Net benefit at 20% threshold	0.145	0.168	+0.023
Net benefit at 30% threshold	0.099	0.129	+0.030

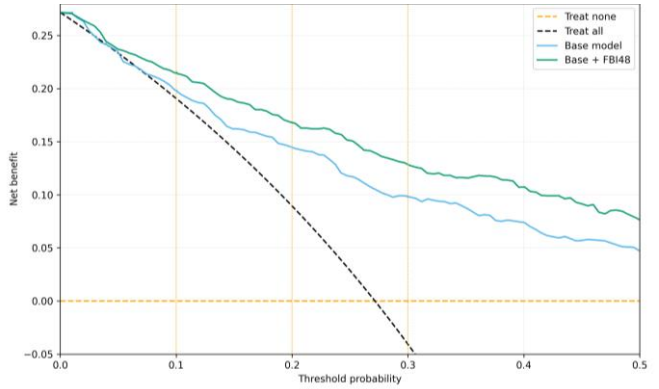

Figure 5. Decision-curve analysis (DCA) for clinical utility. Net benefit across prespecified risk thresholds of 10–30% comparing the base model with the base model plus FBI48. The treat-none and treat-all strategies are shown for reference.

a lower Brier score (0.176 to 0.164; Δ −0.012, p=0.006) (**Figure 4B and Table 3**). The 95% CI for ΔAUC was 0.03–0.07 (DeLong), and the bootstrap 95% CI for the ΔBrier score was −0.019 to −0.005.

Decision-curve analysis showed higher net clinical benefit for the augmented model than for the base model across prespecified triage thresholds, with net-benefit gains of +0.016, +0.023, and +0.030 at 10%, 20%, and 30% risk, respectively, and consistently better performance than a treat-none strategy throughout the 10–30% range (**Figure 5 and Table 3**).

Secondary outcome (SMPP alone). FBI48 also predicted incident SMPP (aOR 1.58 per 1 SD, 95% CI 1.21–2.06), alongside lower SpO2 (aOR 1.22 per 1% lower, 95% CI 1.12–1.34) and moderate/severe imaging (aOR 2.34, 95% CI 1.24–4.40). LDH showed a borderline association (aOR 1.09 per 100 U/L, 95% CI 1.00–1.19), whereas NLR and age were not statistically significant (p≥0.09) (**Supplementary Table S4**). The SMPP model exhibited strong apparent discrimination (AUC 0.85, 95% CI 0.80–0.90), with an optimism-corrected AUC of 0.84, near-ideal calibration (slope 1.01), and a Brier score of 0.090. Bootstrap internal validation used 1000 resamples for the SMPP model.

Sensitivity analyses. Redefining FBI48 using fever thresholds of 38.5 °C and 39.0 °C yielded similar associations with the composite endpoint (aOR per 1 SD 1.37, 95% CI 1.18–1.61; and 1.31, 95% CI 1.12–1.53, respectively), supporting robustness of the FBI48 signal. Tertile summaries were used for description only and not for model fitting (**Supplementary Table S3 and Figure 2**).

Discussion. Our study found that a higher FBI48 was independently associated with a greater risk of refractory and/or severe evolution of MPP. FBI48 captured risk in a monotonic, mildly nonlinear fashion on restricted cubic splines and added clinically meaningful prognostic

information beyond guideline-consistent admission predictors. These results support FBI48 as a simple pre-admission dynamic metric that complements existing risk markers.

In our cohort of hospitalized children with laboratory-confirmed MPP, a higher FBI48 at admission was independently associated with a greater risk of refractory and/or severe evolution, with parallel gradients in injury and inflammatory biomarkers (LDH, NLR, CRP, PCT). These observations are biologically coherent with pediatric MPP pathophysiology. Contemporary guidelines operationalize RMPP as persistent fever with non-improving/worsening radiology despite ≥7 days of macrolide therapy and define SMPP within pediatric CAP severity criteria, emphasizing a host-inflammatory phenotype.[17] LDH reflects parenchymal injury and consistently tracks the risk of RMPP, including in meta-analytic evidence and early admission cohorts.[18,19] Hematologic and acute-phase markers, higher NLR, CRP, and PCT, associate with worse courses or prolonged fever in pediatric MPP, situating FBI48 as a dynamic summary of sustained inflammatory drive that aligns with these static markers.[14,20,21] Rising macrolide resistance can prolong fever and amplify inflammatory burden in children even when radiographic trajectories vary, further supporting the biological plausibility of a pre-admission fever-derived metric as an early risk signal.[22] Because cytokines (e.g., IL-6, TNF-α) were not routinely measured in this retrospective cohort, the proposed biological link between FBI48 and sustained inflammatory drive is based on prior studies and is not directly demonstrated here.

At the bedside, adding FBI48 to a base model of clinical features and routine laboratories improved discrimination, calibration, and overall accuracy, and yielded higher net benefit across prespecified action thresholds of 10–30%, the range clinicians use to consider escalation on general wards. These thresholds map to guideline-anchored decisions already used in pediatric CAP/MPP—pulse oximetry to guide site-of-care and the routine use of an admission chest radiograph in hospitalized children, reserving CT for complications or non-response.[23,24] DCA is the appropriate lens for translating these gains into practice, and current methodological standards support judging clinical usefulness by net benefit across plausible thresholds. MPP-adjacent work using LDH illustrates such added value with DCA in pneumonia phenotypes.[25-27] For children flagged by higher FBI48 within the 10–30% bands, our results justify earlier imaging review, closer respiratory monitoring, and timely consideration of adjunctive anti-inflammatory therapies. Meta-analyses suggest glucocorticoids shorten fever and hospitalization in macrolide-refractory pediatric MPP, and IVIG plus macrolide may benefit selected refractory cases, though not for routine use in all SMPP presentations.[28,29,30]

FBI48 is readily computable from routine ED/outpatient temperatures and caregiver logs using a standard pediatric fever threshold of ≥38.0 °C, with transparent sensitivity checks at 38.5 °C and 39.0 °C. This is consistent with national guidance on fever assessment in children and with pediatric practice reviews.[31,32] Because measurement site and device affect recorded values, harmonization is essential: peripheral methods (tympanic/temporal/axillary) are widely used and can support screening, but they show predictable bias and wider limits of agreement versus rectal/core measures, reinforcing our analytic choice to align units, time-stamp readings, perform linear interpolation only between observed points, and avoid extrapolation beyond the observed window when computing FBI48.[33,34] These steps allow teams to operationalize FBI48 with minimal workflow burden and to embed the metric into admission-time risk calculators or EHR-based triage prompts for pediatric MPP.

Limitations of our study include a retrospective design, possible measurement error in caregiver-recorded temperatures, mixed thermometer sites, and a single-center case mix, which may limit generalizability. Requiring analyzable −48 to 0 h temperature data and a complete admission laboratory panel may introduce selection bias by preferentially including children with more complete monitoring and diagnostic workup. Residual confounding cannot be excluded, and operational definitions of SMPP may vary across institutions despite our prespecification, potentially leading to outcome misclassification. Testing for non-mycoplasma respiratory pathogens was not systematic, so unrecognized viral or bacterial coinfection could partially confound fever trajectories and outcomes. Macrolide-resistance testing was not routinely available; therefore, we could not quantify local resistance rates or evaluate effect modification by resistance status, and generalizability to settings with different resistance epidemiology remains uncertain. Although included and excluded eligible hospitalizations were similar on available baseline variables, selection bias from documentation requirements cannot be fully excluded. Radiographic severity was abstracted from routine radiology reports, and we did not perform a formal inter-rater reliability study. Our models were internally, not externally, validated, and the SMPP model, while penalized, still has a modest number of events. Future work should prioritize external validation across diverse centers and epidemic periods. Prospective capture of high-frequency, time-stamped digital temperature streams to reduce measurement noise and enable standardized integration rules; and formal evaluation of time-varying fever-burden indices to test whether dynamic re-estimation further improves early triage decisions and patient-centered outcomes when

embedded in EHR workflows.

In our study, FBI48 provided independent and incremental prognostic information beyond routine admission predictors. Because this was a retrospective single-center analysis without external validation, FBI48 should be viewed as a promising candidate feature for admission-time risk stratification. External validation and prospective impact studies are needed before routine clinical deployment, including heat-to-head comparison with existing pediatric MPP prognostic models and evaluation of whether FBI48 can safely support escalation decisions (e.g., intensified monitoring or consideration of adjunctive anti-inflammatory therapy).

Ethics approval and consent to participate. This study was conducted in accordance with the Declaration of Helsinki. The protocol was reviewed and approved by the Ethics Committee of The Second Affiliated Hospital of Guangdong Medical University, which waived the requirement for informed consent because the study was a retrospective analysis of de-identified, routinely collected data and posed no more than minimal risk to participants. All data were anonymized prior to analysis.

Data availability statement. Data sets generated during the current study are available from the corresponding author on reasonable request.

Author Contribution Statement. The authors confirm contribution to the paper as follows: study conception and design: L.M.; data collection: L.M., L.C.; analysis and interpretation of results: L.M., L.C.; draft manuscript preparation: L.M., L.C. All authors reviewed the results and approved the final version of the manuscript.

References:

1. Chen, Q., Hu, T., Wu, L., & Chen, L. (2024). Clinical Features and Biomarkers for Early Prediction of Refractory Mycoplasma Pneumoniae Pneumonia in Children. Emergency Medicine International, 2024, 9328177. https://doi.org/10.1155/2024/9328177
2. Xu, D., Zhang, A. L., Zheng, J. S., Ye, M. W., Li, F., Qian, G. C., Shi, H. B., Jin, X. H., Huang, L. P., Mei, J. G., Mei, G. H., Xu, Z., Fu, H., Lin, J. J., Ye, H. Z., Zheng, Y., Hua, L. L., Yang, M., Tong, J. M., Chen, L. L.,Wang, Y. S. (2024). Zhonghua er ke za zhi = Chinese Journal of Pediatrics,62(4), 317–322. https://doi.org/10.3760/cma.j.cn112140-20231121-00383
3. Wang, L. P., Hu, Z. H., Jiang, J. S., & Jin, J. (2024). Serum inflammatory markers in children with Mycoplasma pneumoniae pneumonia and their predictive value for mycoplasma severity. World journal of clinical cases, 12(22), 4940–4946. https://doi.org/10.12998/wjcc.v12.i22.4940
4. Yang, S., Liu, X., Wang, H., Li, H., & Li, X. (2024). Ertong zhongzheng feiyan zhiyuantǐ feiyan weixian yinsu de Meta fenxi [Risk factors for severe Mycoplasma pneumoniae pneumonia in children: a meta-analysis]. Zhongguo Quan Ke Yi Xue [Chinese General Practice], 27(14), 1750–1760. https://doi.org/10.12114/j.issn.1007-9572.2023.0737
5. Liu, J. R., Peng, Y., Yang, H. M., Li, H. M., Zhao, S. Y., & Jiang, Z. F. (2012). Zhonghua er ke za zhi = Chinese Journal of Pediatrics, 50(12), 915–918.
6. Tong, L., Huang, S., Zheng, C., Zhang, Y., & Chen, Z. (2022). Refractory Mycoplasma pneumoniae Pneumonia in Children: Early Recognition and Management. Journal of Clinical Medicine, 11(10), 2824. https://doi.org/10.3390/jcm11102824
7. Zhang, X., Sun, R., Jia, W., Li, P., & Song, C. (2024). A new dynamic nomogram for predicting the risk of severe Mycoplasma pneumoniae pneumonia in children. Scientific Reports,14(1), 8260. https://doi.org/10.1038/s41598-024-58784-3
8. Wrotek, S., LeGrand, E. K., Dzialuk, A., & Alcock, J. (2020). Let fever do its job: The meaning of fever in the pandemic era. Evolution, Medicine, and Public Health, 9(1), 26–35. https://doi.org/10.1093/emph/eoaa044
9. Bhavani, S. V., Verhoef, P. A., Maier, C. L., Robichaux, C., Parker, W. F., Holder, A., Kamaleswaran, R., Wang, M. D., Churpek, M. M., & Coopersmith, C. M. (2022). Coronavirus disease 2019 temperature trajectories correlate with hyperinflammatory and hypercoagulable subphenotypes. Critical Care Medicine, 50(2), 212–223. https://doi.org/10.1097/CCM.0000000000005397
10. Fekety, F. R., Jr, & McDaniel, E. (1968). The fever index in evaluation of the course of infectious diseases, with special reference to pneumococcal pneumonia.The Yale Journal of Biology and Medicine,41(3), 282–288.
11. Balanza, N., Erice, C., Ngai, M., Varo, R., Kain, K. C., & Bassat, Q. (2020). Host-Based Prognostic Biomarkers to Improve Risk Stratification and Outcome of Febrile Children in Low- and Middle-Income Countries. Frontiers in Pediatrics, 8, 552083. https://doi.org/10.3389/fped.2020.552083
12. Miller, A. C., Koeneman, S. H., Suneja, M., Cavanaugh, J. E., & Polgreen, P. M. (2023). Diurnal temperature variation and the implications for diagnosis and infectious disease screening: a population-based study. Diagnosis (Berlin, Germany), 11(1), 54–62. https://doi.org/10.1515/dx-2023-0074
13. Sjauw, K. D., van der Horst, I. C., Nijsten, M. W., Nieuwland, W., & Zijlstra, F. (2006). Value of routine admission laboratory tests to predict thirty-day mortality in patients with acute myocardial infarction. The American Journal of Cardiology, 97(10), 1435–1440. https://doi.org/10.1016/j.amjcard.2005.12.034
14. Li, D., Gu, H., Chen, L., Wu, R., Jiang, Y., Huang, X., Zhao, D., & Liu, F. (2023). Neutrophil-to-lymphocyte ratio as a predictor of poor outcomes of Mycoplasma pneumoniae. Frontiers in Immunology,14, 1302702. https://doi.org/10.3389/fimmu.2023.1302702
15. Steyerberg, E. W., & Vergouwe, Y. (2014). Towards better clinical prediction models: seven steps for development and an ABCD for validation. European Heart Journal, 35(29), 1925–1931. https://doi.org/10.1093/eurheartj/ehu207
16. Sutch, S., Lemke, K., & Abrams, C. (2015). Predictive models of the risk of hospital admission and re-admission: Current and future development. BMC Health Services Research, 15(Suppl 2), A9. https://doi.org/10.1186/1472-6963-15-S2-A9
17. Subspecialty Group of Respiratory, the Society of Pediatrics, Chinese Medical Association, China National Clinical Research Center of Respiratory Diseases, & Editorial Board, Chinese Journal of Pediatrics (2025). Evidence-based guideline for the diagnosis and treatment of Mycoplasma pneumoniae in children (2023). Pediatric Investigation,9(1), 1–11. https://doi.org/10.1002/ped4.12469
18. Wang, S., Jiang, Z., Li, X., Sun, C., Zhang, Y., & Xiao, Z. (2023). Diagnostic value of serum LDH in children with refractory Mycoplasma pneumoniae pneumoniae: A systematic review and meta-analysis. Frontiers in Pediatrics,11, 1094118. https://doi.org/10.3389/fped.2023.1094118
19. Lu, A., Wang, C., Zhang, X., Wang, L., & Qian, L. (2015). Lactate Dehydrogenase as a Biomarker for Prediction of Refractory Mycoplasma pneumoniae Pneumonia in Children. Respiratory Care,60(10), 1469–1475. https://doi.org/10.4187/respcare.03920
20. Nagoba, B. S., Dhotre, S. V., Gavkare, A. M., Mumbre, S. S., & Dhotre, P. S. (2024). Understanding serum inflammatory markers in pediatric Mycoplasma pneumoniae. World Journal of Clinical Pediatrics,13(4), 98809. https://doi.org/10.5409/wjcp.v13.i4.98809
21. Pan, T., Guo, X., Yang, D., Ding, J., & Chen, C. (2024). Expression and

significance of procalcitonin, leukotriene B4, serum amyloid A, and C-reactive protein in children with different types of pneumonia: An observational study. Medicine,103(19), e37817. https://doi.org/10.1097/MD.0000000000037817
22. Yun K. W. (2025). Growing Threat of Macrolide-Resistant Mycoplasma pneumoniae Among Children: What We Know and What We Need. Journal of Korean Medical Science,40(43), e317. https://doi.org/10.3346/jkms.2025.40.e317
23. Bradley, J. S., Byington, C. L., Shah, S. S., Alverson, B., Carter, E. R., Harrison, C., Kaplan, S. L., Mace, S. E., McCracken, G. H., Jr, Moore, M. R., St Peter, S. D., Stockwell, J. A., Swanson, J. T., & Pediatric Infectious Diseases Society and the Infectious Diseases Society of America (2011). Executive summary: the management of community-acquired pneumonia in infants and children older than 3 months of age: clinical practice guidelines by the Pediatric Infectious Diseases Society and the Infectious Diseases Society of America .Clinical Infectious Diseases: an official publication of the Infectious Diseases Society of America,53(7), 617–630. https://doi.org/10.1093/cid/cir625
24. Andronikou, S., Lambert, E., Halton, J., Hilder, L., Crumley, I., Lyttle, M. D., & Kosack, C. (2017). Guidelines for the use of chest radiographs in community-acquired pneumonia in children and adolescents. Pediatric Radiology, 47(11), 1405–1411. https://doi.org/10.1007/s00247-017-3944-4
25. Vickers, A. J., & Elkin, E. B. (2006). Decision curve analysis: a novel method for evaluating prediction models. Medical Decision Making: an International Journal of the Society for Medical Decision Making,26(6), 565–574. https://doi.org/10.1177/0272989X06295361
26. Vickers, A. J., van Calster, B., & Steyerberg, E. W. (2019). A simple, step-by-step guide to interpreting decision curve analysis. Diagnostic and Prognostic Research, 3, 18. https://doi.org/10.1186/s41512-019-0064-7
27. Yanhong, R., Shuai, Z., Dan, C., & Xiaomin, S. (2024). Predictive value of lactate dehydrogenase for Mycoplasma pneumoniae necrotizing pneumonia in children based on decision curve analysis and dose-response analysis. Scientific Reports,14(1), 9803. https://doi.org/10.1038/s41598-024-60359-1
28. Yan H., Zhang C. Dynamic multiplex cytokine profiling to identify risk factors for lung consolidation and necrotizing transformation in children with Mycoplasma pneumoniae pneumonia. Mediterr J Hematol Infect Dis 2026, 18(1): e2026008 https://doi.org/10.4084/MJHID.2026.008 PMid:41641392 PMCid:PMC12867024
29. Kim, H. S., Sol, I. S., Li, D., Choi, M., Choi, Y. J., Lee, K. S., Seo, J. H., Lee, Y. J., Yang, H. J., & Kim, H. H. (2019). Efficacy of glucocorticoids for the treatment of macrolide refractory mycoplasma pneumonia in children: meta-analysis of randomized controlled trials. BMC Pulmonary Medicine,19(1), 251. https://doi.org/10.1186/s12890-019-0990-8
30. Shen, Y. Y., Feng, Z. Q., Wang, Z. P., Wang, X. Q., Luo, C., & Liu, Q. Z. (2024). Efficacy of azithromycin combined with intravenous immunoglobulin in the treatment of refractory mycoplasma pneumoniae pneumonia in children: a meta-analysis. BMC Pediatrics,24(1), 678. https://doi.org/10.1186/s12887-024-05150-x
31. National Institute for Health and Care Excellence. (2019). Fever in under 5s: Assessment and Initial Management [NICE Guideline No. 143]. https://www.nice.org.uk/guidance/ng143
32. Hamilton, J. L., Evans, S. G., & Bakshi, M. (2020). Management of Fever in Infants and Young Children. American Family Physician, 101(12), 721–729.
33. Shi, D., Zhang, L. Y., & Li, H. X. (2020). Diagnostic test accuracy of new generation tympanic thermometry in children under different cutoffs: a systematic review and meta-analysis. BMC Pediatrics,20(1), 210. https://doi.org/10.1186/s12887-020-02097-718
34. Alayed, Y., Kilani, M. A., Hommadi, A., Alkhalifah, M., Alhaffar, D., & Bashir, M. (2022). Accuracy of the Axillary Temperature Screening Compared to Core Rectal Temperature in Infants .Global Pediatric Health, 9, 2333794X221107481. https://doi.org/10.1177/2333794X221107481